Tunable control of the frequency correlations of entangled photons

M. Hendrych,* M. Mičuda, and J. P. Torres

ICFO-Institut de Ciencies Fotoniques, and Department of Signal Theory and Communications, Universitat Politecnica de Catalunya, Castelldefels, 08860 Barcelona, Spain

**Corresponding author: martin.hendrych@icfo.es*

Received April 17, 2007; revised June 14, 2007; accepted June 17, 2007; posted June 28, 2007 (Doc. ID 82108); published August 2, 2007

We experimentally demonstrate a new technique to control the type of frequency correlations of entangled photon pairs generated by spontaneous parametric downconversion. Frequency-correlated and frequency-anticorrelated photons are produced when a broadband pulse is used as a pump. The method is based on the control of the group velocities of the interacting waves and can be applied in any nonlinear medium and frequency band of interest. © 2007 Optical Society of America

OCIS codes: 270.5290, 270.0270, 190.4410.

One of the goals of quantum optics is to implement new sources of quantum light that allow tunable control of the relevant photonic properties. The most appropriate type of frequency correlations between paired photons depends on the specific quantum information application under consideration. Some protocols for quantum enhanced clock synchronization and position measurement rely on the use of frequency-correlated photons [1]. Heralded single photons with a high degree of quantum purity can be obtained by a generation of frequency-uncorrelated paired photons [2]. The use of frequency-correlated (anticorrelated) photons allows the erasing of the distinguishing information coming from the spectra when considering polarization entanglement.

The most widely used method for the generation of pairs of entangled photons is spontaneous parametric downconversion (SPDC). SPDC with continuous-wave pumping produces frequency-anticorrelated photons. Nevertheless, many applications require ultrashort pulses, and under such conditions the frequency anticorrelation is lost. Other specific frequency correlations, such as correlated or uncorrelated photons, can occur in special crystals with suitable pump-light conditions and dispersive properties of the nonlinear crystals [3,4].

It has been shown that noncollinear SPDC allows the generation of frequency-correlated and uncorrelated photons by controlling the pump-beam width and the angle of emission of the downconverted photons [5,6]. Nonlinear crystal superlattices enable the control of frequency correlations as well [7].

In this Letter we experimentally demonstrate a new technique to tailor the frequency correlations of entangled photons [8], which makes it possible to generate frequency-correlated, anticorrelated, and even uncorrelated entangled photon pairs. The method is based on the proper tailoring of the group velocities of all interacting waves through the use of beams with angular dispersion, i.e., pulses with pulse-front tilt. Importantly, this technique works independently of the working frequency band and the nonlinear crystal used, and therefore it can be implemented in materials and frequency bands where conventional solutions do not hold. The scheme allows one to easily tune the frequency correlations by changing only the amount of the angular dispersion of the pump beam, with no further changes of the SPDC source.

Let us consider a collinear SPDC configuration with type-II (*oee*) phase matching. The input pump beam with a central angular frequency ω_p passes through a medium with angular dispersion, such as a diffraction grating oriented along the transverse x direction. The transformation of the pump beam that is due to the grating can be written as [9] $E_p(\omega_p+\Omega_p,p_x,p_y) \Rightarrow E_p(\omega_p+\Omega_p,p_x/\alpha - \Omega_p \tan\phi/(\alpha c),p_y)$, where Ω_p is the angular frequency deviation, $\mathbf{p}=(p_x,p_y)$ is the transverse wave vector, $\alpha=-\cos\theta_0/\cos\beta_0$, θ_0 is the angle of incidence at the grating, β_0 is the output diffraction angle, and c is the speed of light.

The resulting beam acquires a pulse-front tilt such that its peak intensity is located at a different time for each value of x. The tilt angle is $\tan\phi=-\lambda_p\epsilon$, where $\epsilon=m/(d\cos\beta_0)$ is the angular dispersion with d being the groove spacing of the grating, m the diffraction order, and $\lambda_p=2\pi c/\omega_p$. At the output face of the nonlinear crystal, a second grating is used to recollimate the beam by compensating for the angular dispersion introduced by the first grating.

The quantum state of the downconverted photons is $|\Psi\rangle=\int d\Omega_s d\Omega_i \Phi(\Omega_s,\Omega_i)|\omega_s+\Omega_s\rangle_s|\omega_i+\Omega_i\rangle_i$, where [8]

$$\Phi(\Omega_s,\Omega_i) = E_p(\Omega_s+\Omega_i)\mathrm{sinc}(\Delta_k L/2) \times \exp(is_k L/2)\mathcal{F}(\Omega_s)\mathcal{F}(\Omega_i), \quad (1)$$

and $\Delta_k=k_p-k_s-k_i$, $s_k=k_p+k_s+k_i$, $k_j=[(\omega_j+\Omega_j)^2 n_j^2/c^2 - (\Omega_j\tan\phi/c)^2]^{1/2}$, $\omega_p=\omega_s+\omega_i$, $\Omega_p=\Omega_s+\Omega_i$, and $\mathcal{F}$ are interference filters in front of the detectors. The photons are projected into $\mathbf{p}=0$, $\mathbf{q}=0$.

The effective inverse group velocity of all interacting waves is [10] $u_j=N_j+\tan\rho_j\tan\phi/c$, and the effective inverse group velocity dispersion is $g_j=D_j-[\tan\phi/c]^2/k_j$, where ρ_j is the Poynting vector walkoff, k_j is the longitudinal wave number, and N_j

0146-9592/07/162339-3/$15.00

and D_j are the corresponding inverse group velocity and group velocity dispersion parameters, respectively.

The joint spectral amplitude $\Phi(\Omega_s,\Omega_i)$ is mainly determined by the spectral shape of the pump beam and the relationship between all the group velocities [3]. For equal effective group velocities ($u_s=u_i$), one obtains photons highly anticorrelated in frequency ($\Omega_s=-\Omega_i$). For $u_p=(u_s+u_i)/2$, the so-called group velocity matching condition [11], the pair of photons is highly correlated in frequency ($\Omega_s=\Omega_i$). If we define two spectral intensities in the directions $\Omega_\pm=\Omega_s\pm\Omega_i$, $S_\pm(\Omega_\pm)=\int d\Omega_\pm|\Phi(\Omega_+,\Omega_-)|^2$, frequency-anticorrelated (correlated) photons correspond to the case where the bandwidth of S_+ is much narrower (wider) than the bandwidth of S_-.

For a tilt angle

$$\phi=\tan^{-1}\left\{\frac{c(N_i-N_s)}{\tan\rho_s-\tan\rho_i}\right\}, \tag{2}$$

the condition $u_s=u_i$ is fulfilled. S_+ and S_- are written

$$S_+(\Omega_+)=|E_p(\Omega_+)|^2\,\mathrm{sinc}^2(D_+L\Omega_+/2)\mathcal{F}(\Omega_+),$$

$$S_-(\Omega_-)=\mathrm{sinc}^2[(g_s+g_i)L\Omega_-^2/16]\mathcal{F}(\Omega_-), \tag{3}$$

where $D_+=u_p-(u_s+u_i)/2$. The corresponding theoretical joint spectral intensity plotted in Fig. 1(a) shows high frequency anticorrelation.

The tilt required for the generation of highly frequency-correlated photons shown in Fig. 1(b) is written

$$\phi=\tan^{-1}\left\{\frac{c(2N_p-N_s-N_i)}{\tan\rho_s+\tan\rho_i-2\tan\rho_p}\right\}, \tag{4}$$

and the corresponding spectral intensities are

$$S_+(\Omega_+)=|E_p(\Omega_+)|^2\mathcal{F}(\Omega_+),$$

$$S_-(\Omega_-)=\mathrm{sinc}^2[(u_s-u_i)L\Omega_-/4]\mathcal{F}(\Omega_-). \tag{5}$$

We set up an experiment (see Fig. 2) to demonstrate the feasibility of the technique described here. The second harmonic beam (500 mW of average power, 76 MHz repetition rate) of a femtosecond Ti:sapphire laser tuned at 810 nm is directed at a diffraction grating (Gr1) that introduces the appropriate amount of pulse-front tilt (ϕ) in the plane determined by the pump-beam direction of propagation and the optic axis of the nonlinear crystal. The measured bandwidth of the pump beam was $\Delta\lambda_p=3.6$ nm (FWHM). The pulses diffracted off the grating enter a 2 mm thick β-barium borate (BBO) crystal where degenerate collinear type-II SPDC occurs. After the downconversion process, the angular dispersion of the downconverted photons is removed by an inverse grating (Gr2).

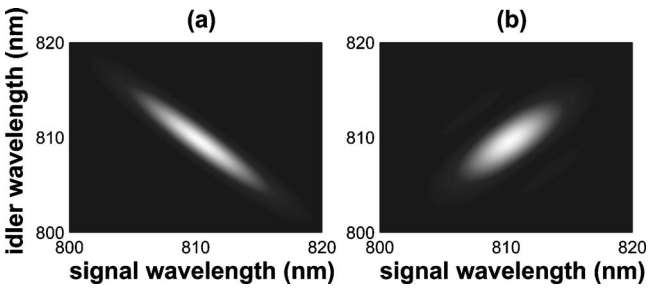

Fig. 1. Joint spectral intensity (theory) for (a) high frequency anticorrelation ($\phi=38.1°$) and (b) high frequency correlation ($\phi=-51.9°$).

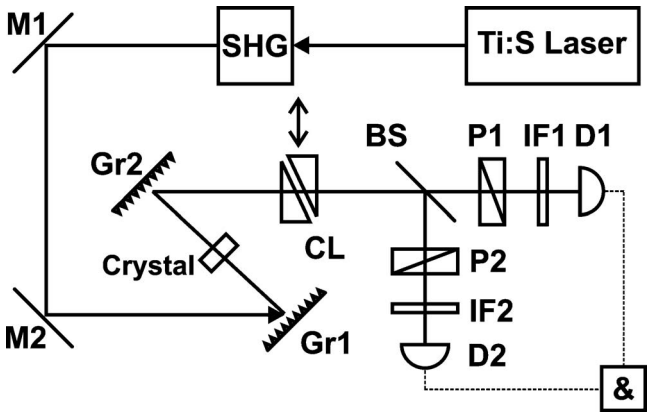

Fig. 2. Experimental setup. SHG, second harmonic generation; M, mirrors; Gr, gratings; CL, compensation line; BS, beamsplitter; P, polarizers; IF, interference filters; D, detectors; &, coincidence electronics.

To evaluate the different types of frequency correlations and the bandwidth, a Hong–Ou–Mandel (HOM) interferometer is used [12,13]. A variable polarization-dependent delay line made of birefringent quartz is inserted between the nonlinear crystal and the beam splitter, which allows us to add a variable time delay (τ) between the generated paired photons. After the beam splitter, polarizers (P) are used to control the polarization of the photons. There are 10 nm (FWHM) interference filters in front of single-photon counting modules where the coincident arrival of two photons in a time window of $\simeq$12 ns is measured.

The coincidence rate $R(\tau,\theta_a=-45°,\theta_b=45°)$, where $\theta_{a,b}$ are the angles of the two polarizers, is given by

$$R(\tau)=\frac{1}{2}\left[1-\frac{1}{2}\int \mathrm{d}\Omega_- S_0(\Omega_-)\exp(-i\Omega_-\tau)\right], \tag{6}$$

where $S_0(\Omega_-)=\int \mathrm{d}\Omega_+\Phi(\Omega_+,\Omega_-)\Phi^*(\Omega_+,-\Omega_-)$.

Figure 3 shows our main experimental results. The normalized number of coincidences (for the sake of comparison) is plotted versus the time delay introduced by the delay line. When no tilt is applied to the pump pulse ($\phi=0°$), the visibility $V=(R_{max}-R_{min})/(R_{max}+R_{min})$ of the HOM dip drops to $V=38\%$. The degradation of the frequency anticorrelation due to the broadband pump beam introduces distinguishing information between the ordinary and extraordinary downconverted photons. The center of the dip is located at $\tau_0=(N_s-N_i)L/2$ [14].

The tilt angle for anticorrelated photons is $\phi=38.1°$, and one has $S_0(\Omega_-)=S_-(\Omega_-)$ and $\tau_0=0$. This amount of angular dispersion is introduced by a grat-

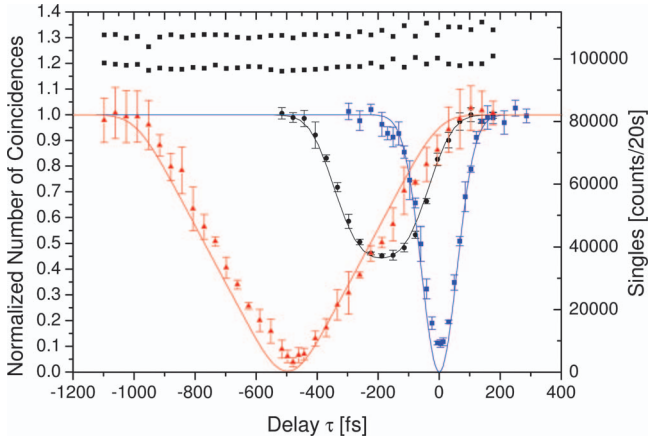

Fig. 3. Normalized number of coincidences and singles as a function of time delay in a HOM interferometer for three different values of the tilt angle (ϕ). Circles, no pulse-front tilt ($\phi=0°$); squares, highly frequency-anticorrelated photons ($\phi=38.1°$); triangles, highly frequency-correlated photons ($\phi=-51.9°$); black squares, singles counts. Solid curves are the theoretical prediction. The experimental points are raw data without any corrections for measurement noise.

ing of 1200 lines/mm and a diffraction order of $m=-1$. Grating Gr2 then has 600 lines/mm and $m=-1$. The measured visibility of the HOM dip is now 83%. Importantly, notice that we generate highly anticorrelated photons even when a broadband pump beam is used.

The generation of highly correlated photons requires a tilt angle $\phi=-51.9°$. The spectral intensity is written $S_0(\Omega_-)=S_-(\Omega_-)\exp[i(u_s-u_i)L/2]$, and $\tau_0=(u_s-u_i)L/2$. A grating Gr1 with 2400 lines/mm and $m=1$, and Gr2 with 1200 lines/mm and $m=1$ are used. The visibility of the HOM dip goes up to 93%. Now the shape of the dip is triangular due to the type-II-like spectral intensity $S_-(\Omega_-)$ given by Eq. (5). Typical values of the measured numbers of coincidences were 6000, 300, and 100 counts/min in the case of no tilt, anticorrelated, and correlated photons, respectively.

Under our experimental conditions, the polarization two-photon state is written $|\Psi\rangle=\varepsilon|\psi\rangle\langle\psi| + (1-\varepsilon)/2\{|H\rangle_s|V\rangle_i\langle H|_s\langle V|_i + |V\rangle_s|H\rangle_i\langle V|_s\langle H|_i\}$, where $|\psi\rangle = 1/\sqrt{2}\{|H\rangle_s|V\rangle_i + \exp(i\Delta)|V\rangle_s|H\rangle_i\}$. The purity of the state is $P=(1+\varepsilon^2)/2$ and the visibility of $R(\tau_0,\theta_a=-45°,\theta_b)$ is $V=\varepsilon|\cos\Delta|$.

Figure 4(a) shows $R(\tau_0,\theta_a=-45°,\theta_b)$ for frequency-anticorrelated photons. The corresponding case with no tilt is also shown for comparison. The visibility increases from 58% (no tilt) to 88%. Figure 4(b) shows the case for correlated photons with $\theta_a=-45°$ and $-30°$. The visibility goes up to 95% in both cases. Thus the purity of the state is greater than 0.95.

In conclusion, we have shown that the use of pulse-front tilt allows the tailoring of the frequency correlations of entangled photons. This technique can be used in any nonlinear crystal and frequency band of interest. Pulses with pulse-front tilt are an important and enabling tool in nonlinear optics [15–17]. We add the use of tilted pulses to the toolkit of available techniques in quantum optics for the full control of the properties of photons.

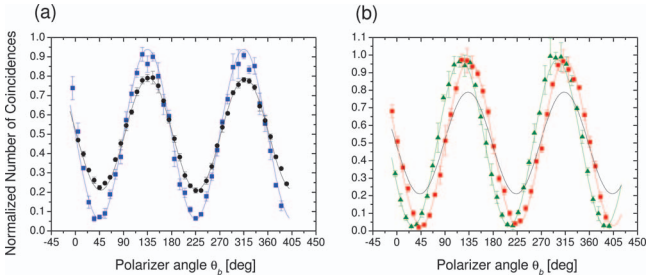

Fig. 4. Coincidence rate as a function of the polarizer angle θ_b. (a) Squares: highly anticorrelated photons. Circles: no tilt. (b) Squares: highly correlated photons with $\theta_a=-45°$ and triangles with $\theta_a=-30°$; black curve: no tilt. Solid curves are $\sin^2$ fits to the raw experimental data.

This work has been supported by EC (QAP, IST directorate, 015848), Government of Spain (Consolider Ingenio 2010 QOIT CSD2006-00019, FIS2004-03556), Government of Catalonia (MH, JPT), and project Center of Modern Optics (LC06007) of Czech Ministry of Education (MM).

References

1. V. Giovannetti, S. Lloyd, and L. Maccone, Science **306**, 1330 (2004).
2. T. Aichele, A. I. Lvovsky, and S. Schiller, Eur. Phys. J. D **18**, 237 (2002).
3. W. P. Grice, A. B. U'Ren, and I. A. Walmsley, Phys. Rev. A **64**, 063815 (2001).
4. O. Kuzucu, M. Fiorentino, M. A. Albota, F. N. C. Wong, and F. X. Kärtner, Phys. Rev. Lett. **94**, 083601 (2005).
5. Z. D. Walton, M. C. Booth, A. V. Sergienko, B. E. A. Saleh, and M. C. Teich, Phys. Rev. A **67**, 053810 (2003).
6. A. B. U'Ren, K. Banaszek, and I. A. Walmsley, Quantum Inf. Comput. **3**, 480 (2003).
7. A. B. U'Ren, R. K. Erdmann, M. de la Cruz-Gutierrez, and I. A. Walmsley, Phys. Rev. Lett. **97**, 223602 (2006).
8. J. P. Torres, F. Macià, S. Carrasco, and L. Torner, Opt. Lett. **30**, 314 (2005).
9. O. E. Martínez, J. Opt. Soc. Am. B **3**, 929 (1986).
10. J. P. Torres, S. Carrasco, L. Torner, and E. W. VanStryland, Opt. Lett. **25**, 1735 (2000).
11. T. E. Keller and M. H. Rubin, Phys. Rev. A **56**, 1534 (1997).
12. C. K. Hong, Z. Y. Ou, and L. Mandel, Phys. Rev. Lett. **59**, 2044 (1987).
13. J. P. Torres, M. W. Mitchell, and M. Hendrych, Phys. Rev. A **71**, 022320 (2005).
14. M. H. Rubin, D. N. Klyshko, Y. H. Shih, and A. V. Sergienko, Phys. Rev. A **50**, 5122 (1994).
15. O. E. Martínez, IEEE J. Quantum Electron. **25**, 2464 (1989).
16. P. Di Trapani, D. Caironi, G. Valiulis, A. Dubietis, R. Danielius, and A. Piskarskas, Phys. Rev. Lett. **81**, 570 (1998).
17. X. Liu, L. J. Qian, and F. W. Wise, Phys. Rev. Lett. **82**, 4631 (1999).